Original Article

Left and right ventricular myocardial deformation and late gadolinium enhancement: incremental prognostic value in amyloid light-chain amyloidosis

Xiao Li[1#], Jian Li[2#], Lu Lin[1], Kaini Shen[2], Zhuang Tian[3], Jian Sun[4], Congli Zhang[2], Jing An[5], Zhengyu Jin[1], Rozemarijn Vliegenthart[6], Joseph B. Selvanayagam[7], Yining Wang[1]

[1]Department of Radiology, [2]Department of Hematology, [3]Department of Cardiology, [4]Department of Pathology, Peking Union Medical College Hospital, Chinese Academy of Medical Sciences & Peking Union Medical College, Beijing, China; [5]Siemens Shenzhen Magnetic Resonance Ltd., Siemens MRI Center, Hi-Tech Industrial Park, Shenzhen, China; [6]Department of Radiology, University Medical Center Groningen, University of Groningen, Groningen, The Netherlands; [7]Department of Cardiovascular Medicine, Flinders University, Flinders Medical Centre, Adelaide, SA, Australia

Contributions: (I) Conception and design: X Li, Y Wang; (II) Administrative support: Z Jin; (III) Provision of study materials or patients: J Li; (IV) Collection and assembly of data: L Lin, K Shen, Z Tian, J Sun; (V) Data analysis and interpretation: C Zhang, R Vliegenthart, JB Selvanayagam; (VI) Manuscript writing: All authors; (VII) Final approval of manuscript: All authors.

[#]These authors contributed equally to this work.

Correspondence to: Yining Wang, MD; Zhengyu Jin, MD. Department of Radiology, Peking Union Medical College Hospital, Chinese Academy of Medical Sciences & Peking Union Medical College, No.1, Shuaifuyuan, Dongcheng District, Beijing 100730, China.
Email: wangyining@pumch.cn; jin_zhengyu@163.com.

Background: Previous cardiac magnetic resonance (CMR) studies have shown that both late gadolinium enhancement (LGE) and left ventricular (LV) strain have prognostic value in amyloid light-chain (AL) amyloidosis, but the right ventricular (RV) strain has not yet been studied. We aim to determine the incremental prognostic value of LV and RV LGE and strain in AL amyloidosis.

Methods: This prospective study recruited 87 patients (age, 56.9±9.1 years; *M*/F, 56/31) and 20 healthy subjects (age, 52.7±8.1 years; *M*/F, 11/9) who underwent CMR. The LV LGE was classified into no, patchy and global groups. The RV LGE was classified into negative and positive groups. Myocardial deformation was measured using a dedicated software. Follow-up was performed for all-cause mortality using Cox proportional hazards regression and Kaplan-Meier curves.

Results: During a median follow-up of 21 months, 34 deaths occurred. Presence of LV LGE [HR 2.44, 95% confidence interval (CI), 1.10–5.45, P=0.029] and global longitudinal strain (GLS) (HR 1.13 per 1% absolute decrease, 95% CI, 1.02–1.25, P=0.025) were independent LV predictors. RV LGE (HR 4.07, 95% CI, 1.09–15.24, P=0.037) and GLS (HR 1.10 per 1% absolute decrease, 95% CI, 1.00–1.21, P=0.047) were independent RV predictors. Complementary to LV LGE, LV GLS impairment or RV LGE further reduced survival (both log rank P<0.001).

Conclusions: This study confirms the incremental prognostic value of LV GLS and RV LGE in AL amyloidosis, which refines the conventional risk evaluation based on LV LGE. GLS based on non-contrast-enhanced CMR are promising new predictors.

Keywords: Amyloidosis; magnetic resonance imaging; cardiomyopathies

Submitted Feb 10, 2020. Accepted for publication Apr 01, 2020.
doi: 10.21037/cdt-20-181
View this article at: http://dx.doi.org/10.21037/cdt-20-181

Introduction

Immunoglobulin amyloid light-chain amyloidosis (AL amyloidosis) is characterized as plasma cell dyscrasia with insoluble immunoglobulin light chain fibrils deposition in various organs and tissues (1). Cardiac involvement is likely underdiagnosed and often misdiagnosed (2,3), while it contributes to approximately one half of early death (4). Therefore, early recognition and close follow-up is of vital importance.

Cardiac magnetic resonance imaging (CMR) offers advantage of precise, comprehensive cardiac structure and function evaluation as well as myocardial tissue characterization. AL amyloidosis typically manifests as increased wall thickness with extensive, predominantly subendocardial late gadolinium enhancement (LGE), not limited to the left ventricle but usually including the right ventricle (5,6). Left ventricular (LV) LGE is proven to be of high diagnostic and prognostic value (7-9). Fewer studies focused on right ventricular (RV) LGE, with inconsistent prognostic results (10,11).

Recently, feature tracking CMR has emerged as a feasible tool for myocardial deformation analysis (12). Cine image-based LV strain is an independent predictor for mortality in AL amyloidosis, even adjusted for LV LGE and ejection fraction (EF) (13,14). The prognostic value of RV longitudinal strain has been demonstrated by echocardiography (15). Since CMR is the reference standard of RV structure and function evaluation, RV strain analyzed by CMR is promising in AL amyloidosis, but has not been reported yet. This study aims to prove the incremental prognostic value of LV and RV myocardial deformation as well as LGE in AL amyloidosis.

Methods

This research was approved by the Institutional Ethnics Committee for Human Research at Peking Union Medical College Hospital (Beijing, China). All subjects have consented to participate in this study.

Study subjects

This prospective study included AL amyloidosis patients who underwent clinical ordered CMR imaging at Peking Union Medical College Hospital between August 1, 2014 and December 31, 2016. Patients with contraindications either to CMR imaging (i.e., CMR-incompatible devices) or contrast administration (i.e., estimated glomerular filtration rate <30 mL/min/1.73 m^2) were excluded (16). Patients who had already received chemotherapy before CMR imaging were also excluded. Eighty-seven patients (age, 56.9±9.1 years; M/F, 56/31) were consecutively recruited. All patients had biopsy evidence of AL amyloidosis based on positive Congo red stain and light chain deposition confirmed by immunohistochemistry, immunofluorescence or mass spectrometer, and 21 had histological evidence of myocardial involvement. All patients underwent laboratory examinations at baseline; serum cardiac biomarkers were used to categorize patients after the revised Mayo staging system (17). Twenty subjects (age, 52.7±8.1 years; M/F, 11/9) who had neither history nor symptoms of cardiovascular diseases were also included as healthy controls.

CMR scanning protocol

CMR was performed on a 3.0 T whole-body MR system (MAGNETOM Skyra, Siemens Healthineers, Erlangen, Germany). An 18-element body matrix coil and a 32-element spine array coil were used for data acquisition. The cine images were acquired with an electrocardiogram-gated 2D balanced steady-state free precession sequence during multiple breath holds. 2-, 3-, and 4-chamber long-axis and 9–11 short-axis slices covering the LV were acquired. Key parameters were as follows: repetition time (TR)/echo time (TE), 3.3/1.43 ms; flip angle (FA), 55°–70°; voxel size, 1.6×1.6×6.0 mm^3; temporal resolution, 45.6 ms; bandwidth, 962 Hz/pixel. LGE images were acquired with a 2D phase-sensitive inversion-recovery (PSIR) gradient-echo pulse sequence 10 minutes after intravenous Gadolinium injection (16). The same long-axis and short-axis slice positions as for cine images were acquired. Segmented approach was applied for all patients, and a motion correction single-shot approach was applied in patients with arrhythmia or poor breath-holding. Parameters of the sequence were as follows: TR/TE/FA, 5.2 ms/1.96 ms/20°; voxel size, 1.4×1.4×8.0 mm^3.

CMR image analysis

CMR images were independently analyzed by two experienced radiologists (3 and 5 years of experience in CMR, respectively). The LV LGE pattern was classified into three categories according to Boynton *et al.* (8) and Fontana *et al.* (9): no LGE, when there were no areas of

LGE; patchy LGE, when there were discrete areas of LGE, or there were diffuse areas of LGE in less than half of the short axis images; global LGE, when there was diffuse, transmural LGE in more than half of the short axis images. The RV LGE pattern was classified into negative and positive. RV LGE imaging was interpreted from the standard acquisition for LV LGE. Isolated RV free wall signal was considered positive. To exclude artifact, LGE was deemed present only if visible in two orthogonal views. Discrepancies were resolved in consensus during a joint evaluation with a third radiologist (14 years of experience).

Cardiac structure, function and myocardial deformation were measured semi-automatically using dedicated CMR software (cvi42, version 5.3, Circle Cardiovascular Imaging, Calgary, Canada), initiated by the automated contour algorithm, then checked and revised manually. Standard parameters of cardiac structure (i.e., ventricular volumes and mass with indexing for body surface area, and atrial volumes) and EF were measured by contouring the endocardial, epicardial and atrial borders on long-axis and short axis cine images at end-systolic and end-diastolic phase (18). Myocardial deformation in longitudinal, radial and circumferential directions were measured by contouring the endocardial and epicardial borders on 2-, 3- and 4-chamber long axis and short axis cine images at the end-diastolic phase. The interventricular septum was considered part of the LV, and the RV trabeculations were regarded as part of the RV cavity volume. In patients without significant RV hypertrophy, endocardial and epicardial borders were defined to allow appropriate tracking points within the myocardial region.

Clinical follow-up

A physician blinded to the results of CMR imaging conducted the telephone and clinical follow-up each month. Unless the outcome was death from any cause, patients were censored at the end of the study follow-up time. If patients were lost to follow-up, their last clinic visit record date was used.

Statistical analysis

Statistical analysis was performed using SPSS Statistics (version 21.0, International Business Machines, Inc., Armonk, New York, USA). The agreement in myocardial deformation parameters between two observers was assessed in 20 randomly selected patients using the intraclass correlation coefficient and Bland-Altman analyses. Correlation between continuous variables or categorical variables was assessed using the Pearson's r correlation or Spearman ρ correlation, respectively. Comparison between patient groups and the control group was performed by one-way analysis of variance (ANOVA) with post-hoc Bonferroni correction. Statistical significance was defined as $P<0.05$. Survival was evaluated with Cox proportional hazards regression analysis, providing estimated hazard ratios (HR) with 95% confidence intervals (CI) and Kaplan-Meier curves. The median value of strain was used as cut-off value.

Results

Baseline characteristics

Table 1 summarizes the characteristics of AL amyloidosis patients and healthy controls at baseline. Patients had lower LVEF and RVEF, as well as higher indexed LV mass and indexed RV mass, compared to healthy controls. Patients showed impaired LV global radial strain (GRS) (41.0%±16.0% *vs.* 60.1%±11.1%, $P<0.001$), global circumferential strain (GCS) (–19.2%±5.1% *vs.* –25.5%±2.2%, $P<0.001$) and global longitudinal strain (GLS) (–12.4%±5.7% *vs.* –21.1%±2.4%, $P<0.001$), as well as RV GRS (22.4%±7.1% *vs.* 26.9%±7.2%, $P=0.011$), GCS (–13.3%±4.4% *vs.* –16.0%±2.7%, $P=0.004$) and GLS (–19.1%±6.3% *vs.* –27.9%±2.3%, $P<0.001$), compared to healthy controls. The intra-observer and inter-observer variability for myocardial deformation parameters are shown in *Table 2*. The Kappa coefficient of classification between the two radiologists was 0.834 for LV LGE, and 0.857 for RV LGE.

Association between LGE and strain values of LV and RV

Representative examples of LGE images and LV strain values from a healthy subject and AL amyloid patients with increasing disease burden are shown in *Figure 1*. LV LGE and RV LGE correlated significantly ($\rho=0.872$, $P<0.001$). The LV strain values in subgroups with different LV LGE patterns are shown in *Figure 2*. LV GRS ($\rho=-0.745$, $P<0.001$), LV GCS ($\rho=0.743$, $P<0.001$) and LV GLS ($\rho=0.805$, $P<0.001$) correlated significantly with LV LGE severity. Patients without LV LGE already had impaired LV GLS (–18.5%±2.8% *vs.* –21.1%±2.4%, $P=0.045$), compared to healthy controls.

Table 1 Baseline characteristics of the AL amyloidosis patients and healthy controls

Characteristics	Patients (n=87)	Healthy controls (n=20)	P
Clinical			
Male/female	56/31	11/9	0.452
Age (years)	56.9±9.1	52.7±8.1	0.050
NYHA (I/II/III/IV)	37/25/21/4	–	–
cTnI (μg/L)	0.047 (0.014–0.127)	–	–
NT-proBNP (pg/mL)	2,094 [309–4,558]	–	–
dFLC (mg/L)	134.4 (60.0–321.3)	–	–
Mayo Stage (I/II/III/IV)	27/18/25/17	–	–
Creatinine (μmol/L)	87.2±35.2	–	–
HTN/CHD/DM/Af	16/7/3/3	–	–
CMR			
Indexed LVEDV (mL/m^2)	77.4±15.3	76.1±8.1	0.601
Indexed LVESV (mL/m^2)	32.6±12.4	22.7±4.1	<0.001**
LVEF (%)	58.4±10.7	70.2±4.3	<0.001**
LA volume (mL)	58.2±27.0	54.1±13.3	0.864
Indexed LV mass (g/m^2)	54.4±19.4	38.1±6.6	<0.001**
LV LGE (none/patchy/extensive)	25/22/40	–	–
LV GRS (%)	41.0±16.0	60.1±11.1	<0.001**
LV GCS (%)	−19.2±5.1	−25.5±2.2	<0.001**
LV GLS (%)	−12.4±5.7	−21.1±2.4	<0.001**
Indexed RVEDV (mL/m^2)	63.3±14.5	71.4±9.6	0.005**
Indexed RVESV (mL/m^2)	27.4±11.3	26.2±4.0	0.968
RVEF (%)	57.2±10.2	63.4±2.5	0.012*
RA volume (mL)	58.6±20.1	58.6±15.6	0.968
Indexed RV mass (g/m^2)	14.0±5.7	10.8±2.1	0.034*
RV LGE (–/+)	39/48	–	–
RV GRS (%)	22.4±7.1	26.9±7.2	0.011*
RV GCS (%)	−13.3±4.4	−16.0±2.7	0.004**
RV GLS (%)	−19.1±6.3	−27.9±2.3	<0.001**

All continuous variables are presented as mean ± SD, except for cTnI, NT-proBNP and dFLC, which are presented as medians (quartiles 1–quartiles 3). *, P<0.05; **, P<0.01. cTnI, cardiac Troponin I; NT-proBNP, N-terminal pro-B-type natriuretic peptide; dFLC, serum immunoglobulin free light chain difference; NYHA, New York Heart Association; HTN, hypertension; CHD, coronary artery heart disease; DM, diabetes mellitus; Af, atrial fibrillation; CMR, cardiac magnetic resonance; LV, left ventricle; RV, right ventricle; EDV, end-diastolic volume; ESV, end-systolic volume; EF, ejection fraction; LGE, late gadolinium enhancement; LA, left atrium; RA, right atrium; GRS, global radial strain; GCS, global circumferential strain; GLS, global longitudinal strain.

Table 2 Intra-observer and inter-observer intraclass correlation coefficient of ventricular strain

	LV GRS	LV GCS	LV GLS	RV GRS	RV GCS	RV GLS
Intra-	0.986	0.993	0.974	0.957	0.908	0.933
Inter-	0.917	0.933	0.928	0.925	0.865	0.919

LV, left ventricle; RV, right ventricle; GRS, global radial strain; GCS, global circumferential strain; GLS, global longitudinal strain.

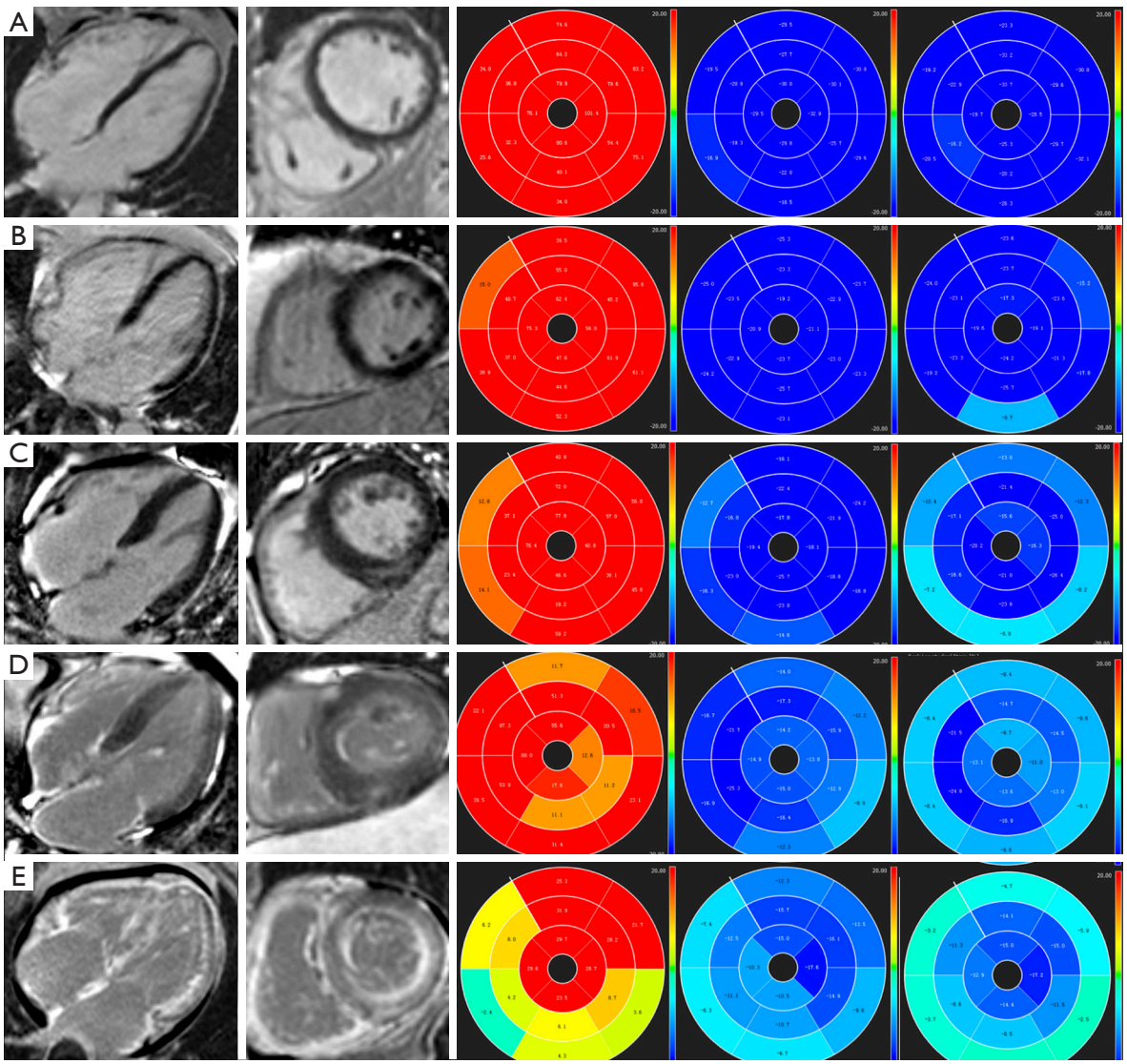

Figure 1 Representative images of LGE images and LV strain values. (A) A healthy subject with negative LGE, a GRS of 63.61%, a GCS of –26.60%, and a GLS of –24.86%. (B) A Mayo Stage I patient with negative LGE, a GRS of 49.35%, a GCS of –22.61% and a GLS of –20.23%. (C) A Mayo Stage II patient with patchy LV LGE, negative RV LGE, a GRS of 40.45%, a GCS of –18.47% and a GLS of –17.51%. (D) A Mayo Stage III patient with patchy LV LGE, positive RV LGE, a GRS of 36.21%, a GCS of –16.53% and a GLS of –15.66%. (E) A Mayo Stage IV patient with extensive LV LGE, positive RV LGE, a GRS of 15.14%, a GCS of –11.65% and a GLS of –9.00%. LV, left ventricular; RV, right ventricular; LGE, late gadolinium enhancement; GRS, global radial strain; GCS, global circumferential strain; GLS, global longitudinal strain.

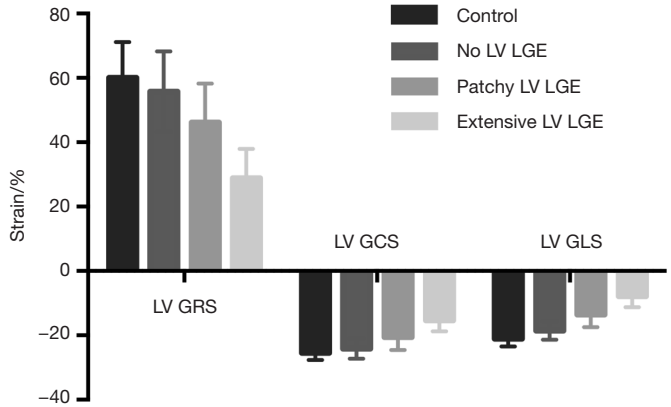

Figure 2 LV strain values with different LV LGE patterns. LV GRS, LV GCS and LV GLS correlated significantly with LV LGE (all P<0.001) severity. Patients without LV LGE had reduced LV GLS (–18.5%±2.8% *vs.* –21.1%±2.4%, P=0.045), compared to healthy controls. LV, left ventricular; LGE, late gadolinium enhancement; GRS, global radial strain; GCS, global circumferential strain; GLS, global longitudinal strain.

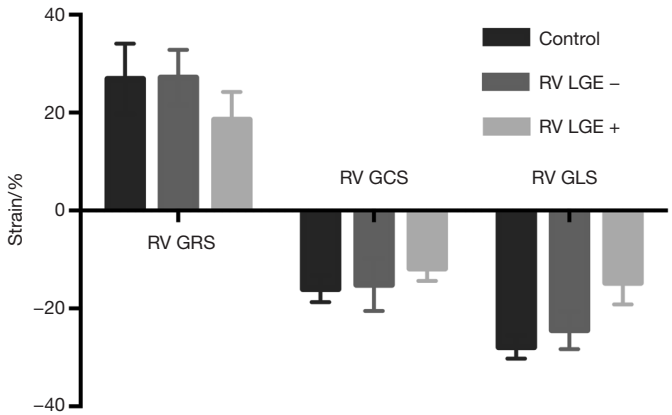

Figure 3 RV strain values with different RV LGE patterns. RV GRS, RV GCS and RV GLS correlated significantly with RV LGE (all P<0.001). Patients without RV LGE had reduced RV GLS (–24.5%±3.8% *vs.* –27.9%±2.3%, P=0.005), compared to healthy controls. RV, right ventricular; LGE, late gadolinium enhancement; GRS, global radial strain; GCS, global circumferential strain; GLS, global longitudinal strain.

The RV strain values in subgroups with different RV LGE patterns are shown in *Figure 3*. RV GRS (ρ=–0.683, P<0.001), RV GCS (ρ=0.619, P<0.001) and RV GLS (ρ=0.763, P<0.001) correlated significantly with RV LGE. Patients without RV LGE already had impaired RV GLS (–24.5%±3.8% *vs.* –27.9%±2.3%, P=0.005), compared to healthy controls.

Association between CMR parameters and clinical stage

Table 3 summarizes the correlation of CMR parameters with Mayo Stage. The EF and mass of LV and RV correlated significantly with Mayo Stage (all P<0.001). The LGE as well as strain parameters of LV and RV correlated significantly with Mayo Stage (all P<0.001). Patients with Mayo Stage I had impaired LV GLS (–17.0%±3.4% *vs.* –21.1%±2.4%, P=0.004) and RV GLS (–23.7%±4.6% *vs.* –27.9%±2.3%, P=0.027), compared to healthy controls.

CMR parameters and clinical outcome

During follow-up, 69 (79.3%) patients received

Table 3 CMR parameters correlation with clinical stage in AL amyloidosis patients

Variable	Control (n=20)	Mayo Stage				Correlation	
		I (n=27)	II (n=18)	III (n=25)	IV (n=17)	ρ	P
LVEF (%)	70.2±4.3	67.0±5.9	59.1±8.4	56.3±10.2	47.2±8.3	−0.649	<0.001
Indexed LV mass (g/m^2)	38.1±6.6	45.1±16.5	50.1±20.8	64.2±19.5	61.0±14.0	0.430	<0.001
LV LGE (no/patchy/extensive)	–	18/8/1	7/5/6	0/7/18	0/2/15	0.726	<0.001
LV GRS (%)	60.1±11.1	54.1±12.6	43.3±14.4	35.0±13.7	26.5±6.2	−0.667	<0.001
LV GCS (%)	−25.5±2.2	−23.5±3.2	−20.4±4.2	−17.0±4.8	−14.3±2.6	0.686	<0.001
LV GLS (%)	−21.1±2.4	−17.0±3.4*	−14.8±5.2	−9.2±3.6	−7.0±3.7	0.707	<0.001
RVEF (%)	63.4±2.5	63.8±6.7	60.0±10.6	55.3±8.5	46.5±6.7	−0.607	<0.001
Indexed RV mass (g/m^2)	10.8±2.1	10.7±3.0	12.9±5.4	16.5±7.0	16.8±4.1	0.489	<0.001
RV LGE (−/+)	–	23/4	10/8	6/19	0/17	0.650	<0.001
RV GRS (%)	26.9±7.2	26.3±6.4	23.7±6.6	21.5±7.0	16.0±4.0	−0.555	<0.001
RV GCS (%)	−16.0±2.7	−14.4±6.2	−14.6±3.0	−13.1±2.9	−10.5±2.2	0.500	<0.001
RV GLS (%)	−27.9±2.3	−23.7±4.6**	−21.4±5.5	−16.3±5.9	−13.5±3.1	0.638	<0.001

Compared with the control, *, P=0.004; **, P=0.027. Correlation was assessed using Spearman ρ correlation. LV, left ventricle; RV, right ventricle; EF, ejection fraction; LGE, late gadolinium enhancement; GRS, global radial strain; GCS, global circumferential strain; GLS, global longitudinal strain.

standardized chemotherapy with thalidomide or bortezomib, cyclophosphamide and dexamethasone (BCD or TCD), 8 (9.2%) received autologous stem cell transplantation, and the remainder did not receive chemotherapy because of the expense or other reasons. At the time of the last follow-up moment, 53 (60.9%) patients were alive, with a survival probability of approximately 64.4% at median follow-up time (21 months); 34 (39.1%) patients were dead, with a median time to death of 5 month. Two patients were lost to follow-up.

Table 4 summarizes the univariate and multivariate Cox proportional hazard analysis of overall survival in all patients. Mayo Stage, LV and RV LGE, LV and RV strain parameters were significantly associated with all-cause mortality in univariate analysis. LV and RV EF, LV and RV mass, and right atrial volume also were predictors. LV LGE and RV LGE were analyzed in separate multivariate Cox models because of a high correlation value (ρ=0.872). LV LGE (HR 2.44, 95% CI, 1.10–5.45, P=0.029) and LV GLS (HR 1.13 per 1% absolute decrease, 95% CI, 1.02–1.25, P=0.025) were independent predictors in a LV parameters based multivariate Cox model. RV LGE (HR 4.07, 95% CI, 1.09–15.24, P=0.037) and RV GLS (HR 1.10 per 1% absolute decrease, 95% CI, 1.00–1.21, P=0.047) were independent predictors in a RV parameters based multivariate Cox model.

For all patients, Kaplan-Meier survival curve showed significant difference in survival probability categorized by LV (*Figure 4A*, 96.0%, 77.3%, and 37.3% at the 21th month respectively, log-rank P<0.001) or RV LGE pattern (*Figure 4B*, 92.3% and 41.3% at the 21th month respectively, log-rank P<0.001). All patients without LV LGE had negative RV LGE; 14/8 patients with patchy LGE had negative/positive RV LGE; all patients with extensive LV LGE had positive RV LGE. Kaplan-Meier survival curve showed RV LGE further reduced survival (*Figure 4C*, 96.0%, 85.7%, 62.5%, and 37.3% at the 21th month respectively, log-rank P<0.001).

We assigned a score of 1 for patchy LV LGE, 2 for extensive LV LGE, and 1 for LV GLS ≥−11.85%, adding together divided patients into four groups with LV Score of 0, 1, 2, and 3, respectively. Kaplan-Meier survival curve showed significant difference in survival probability categorized by LV Score (*Figure 5*, 100.0%, 75.0%, 73.7%, and 34.9% at the 21th month respectively, log-rank P<0.001). Scores based on RV LGE and GLS did not have statistical significance.

Table 4 Univariable and multivariable Cox proportional hazard analysis in AL amyloidosis patients

Variable	Univariable		Multivariable		Multivariable	
	HR (95% CI)	P	HR (95% CI)	P	HR (95% CI)	P
Mayo Stage	1.81 (1.31–2.51)	<0.001	–	–	–	–
LVEF, per unit increase	0.94 (0.91–0.97)	<0.001	–	–		
Indexed LV mass, per unit increase	1.03 (1.01–1.04)	0.001	–	–		
LV LGE	4.25 (2.22–8.14)	<0.001	2.44 (1.10–5.45)	0.029		
LV GRS, per unit increase	0.93 (0.91–0.96)	<0.001	–	–		
LV GCS, per absolute unit decrease	1.18 (1.10–1.27)	<0.001	–	–		
LV GLS, per absolute unit decrease	1.22 (1.13–1.31)	<0.001	1.13 (1.02–1.25)	0.025		
RVEF, per unit increase	0.96 (0.93–0.99)	0.005			–	–
RA volume, per unit increase	1.02 (1.00–1.04)	0.019			–	–
Indexed RV mass, per unit increase	1.08 (1.03–1.13)	0.002			–	–
RV LGE	9.25 (3.24–26.43)	<0.001			4.07 (1.09–15.24)	0.037
RV GRS, per unit increase	0.95 (0.90–1.00)	0.048			–	–
RV GLS, per absolute unit decrease	1.18 (1.10–1.26)	<0.001			1.10 (1.00–1.21)	0.047

All statistically significant prognostic factors in univariate analysis were listed. All clinically and statistically significant variables in univariate analysis were put into the multivariable Cox model. LV LGE and RV LGE were put in separate models because of a correlation ρ=0.872. LV, left ventricle; RV, right ventricle; EF, ejection fraction; LGE, late gadolinium enhancement; RA, right atrium; GRS, global radial strain; GCS, global circumferential strain; GLS, global longitudinal strain; HR, hazard ratio; CI, confidence interval.

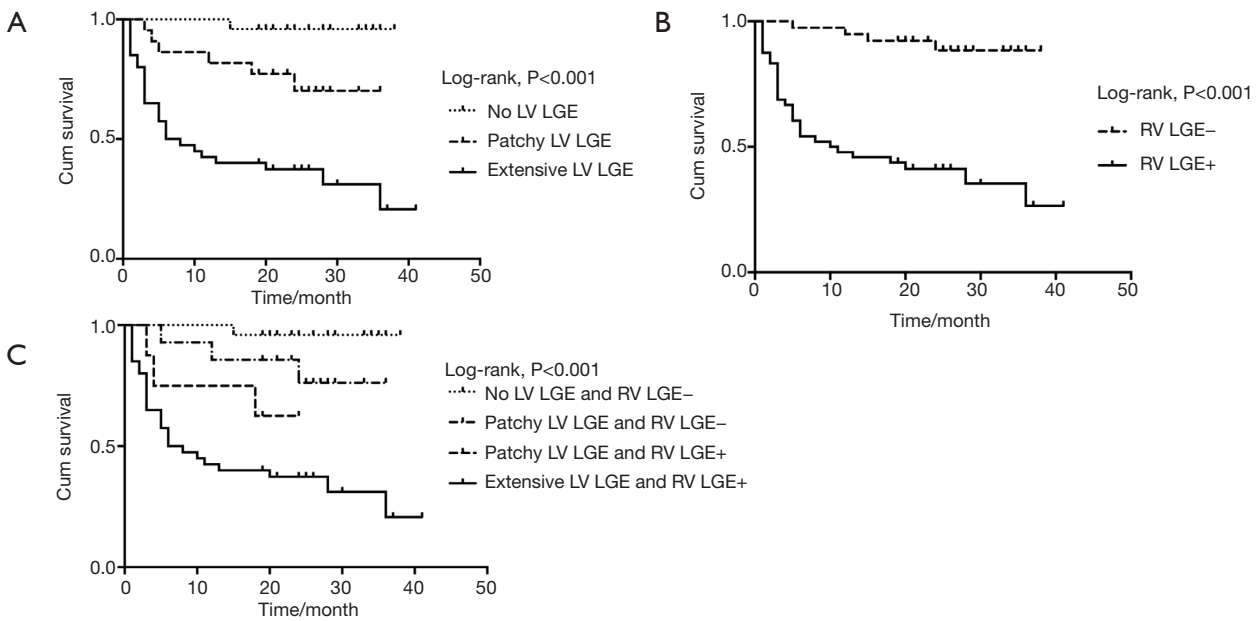

Figure 4 Kaplan-Meier survival curves of LV and RV LGE. (A) Survival probability differed significantly categorized by LV LGE patterns (96.0%, 77.3%, and 37.3% at the 21th month respectively, log-rank P<0.001). (B) Survival probability differed significantly categorized by RV LGE patterns (92.3% and 41.3% at the 21th month respectively, log-rank P<0.001). (C) Survival probability differed significantly categorized by LV and RV LGE patterns (96.0%, 85.7%, 62.5%, and 37.3% at the 21th month respectively, log-rank P<0.001). LV, left ventricular; RV, right ventricular; LGE, late gadolinium enhancement.

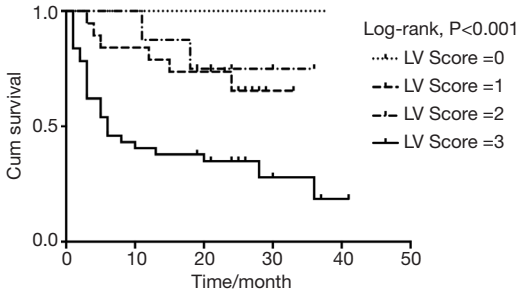

Figure 5 Kaplan-Meier survival curve of LV Score. Patients were divided into four groups with LV Score of 0, 1, 2, and 3, respectively, with 1 for patchy LV LGE, 2 for extensive LV LGE, and 1 for LV GLS ≥–11.85% (median value). Patients categorized by LV Score differed significantly in survival probability (100.0%, 75.0%, 73.7%, and 34.9% at the 21th month respectively, log-rank P<0.001). LV, left ventricular; GLS, global longitudinal strain.

Discussion

Our study has a series of important findings. First, LV and RV strain values correlated significantly with clinical and other imaging parameters of AL amyloidosis disease burden. Second, in patients without serum cardiac biomarkers or LGE evidence of cardiac involvement, LV and RV GLS was already impaired. Third and most importantly, LV and RV LGE and GLS were independent predictors for all-cause mortality in AL amyloidosis. Complementary to LV LGE, LV GLS impairment or RV LGE further reduced survival.

LGE CMR is a classic imaging tool to diagnose cardiac amyloidosis. However, the recognition of LGE lesions involves delineation of abnormal tissue from normal tissue, thus early identification of mild cases or diffuse cardiomyopathy can easily be missed. On the other hand, kidney involvement is common in AL amyloid (19,20), and approximately 15% of patients were excluded in this study because of renal function impairment. Efforts have been made to search for non-contrast-enhanced quantitative parameters, yielding a series of cardiac structural and functional predictors derived from CMR and echocardiography (6,10). Feature tracking CMR based myocardial deformation analysis has attracted increasing attention, as it yields tri-directional strain values from cine-images without additional sequence scanning or contrast injection (12,21). Consistent with previous studies (14,22,23), we proved that LV strain values correlated significantly with clinical and other imaging parameters of AL amyloidosis disease burden, and GLS showed earlier impairment than serum biomarkers, EF or LGE. We and others (13,14) demonstrated that LV strain values are independently prognostic of mortality. The difference was that we and Illman *et al.* (13) found that LV GLS is the independent predictor, while Wan *et al.* (14) found that LV GCS independently predicted mortality. The difference in most predictive strain parameter might due to different vendors or software used and different parameters included.

Another novelty of this study is the evidence of RV parameters for mortality prediction in AL amyloidosis. We demonstrated that RV GLS is an independent predictor, which to our knowledge has not been reported before. Cardiac involvement typically manifests as extensive LGE not limited to the LV but also in the RV (5,24). We validated the prognostic value of LV LGE, consistent with previous important studies (7-9). Fewer data are available regarding the value of RV LGE in AL amyloidosis, which is more difficult to be identified and categorized due to the relatively thin ventricular wall and abundant epicardial fat. Wan *et al.* demonstrated that RV LGE is an independent predictor of mortality (11), while Bodez *et al.* pointed out that plane systolic excursion (TAPSE) derived by echocardiography rather than RV LGE is independently prognostic (10). We proved that RV LGE is an independent predictor over Mayo Stage, RVEF, RV mass and RA volume. Besides, for patients with the same LV LGE pattern, survival probability also differed significantly according to RV LGE pattern. Possible explanations for the difference among studies are different amyloidosis subtypes investigated and different imaging parameters included in the survival analysis.

This study has some limitations. The main limitation is that this is a single-center study. Although we recruited a relatively large patient population and provided good reproducibility of strain values, the results need to be confirmed in other centers with different vendors and analysis methods. Second, we did not perform mortality analysis of cardiovascular events, because many patients, although they got a treatment plan in our hospital, received treatment at their home institution, for whom detailed data of mortality cause is incomplete. Third, we found strain impairment in patients without LGE, but few patients underwent myocardial biopsy. A lack of pathology evidence for cardiac involvement is common with most studies.

Conclusions

This study confirms that strain values based on non-contrast-enhanced CMR are promising early diagnostic

parameters and new predictors for AL amyloidosis, in particular longitudinal strain. Besides, this study highlighted the prognostic value of RV LGE and RV strain values, which refined the conventional risk evaluation based on LV impairment.

Acknowledgments

Funding: This work was supported by the National Natural Science Foundation of China (Grant No. 81901717, for Xiao Li), the National Natural Science Foundation of China (Grant No. 81471725, for Yining Wang), the Beijing Nova of Science and Technology Crossover Project (Z171100001117136, for Yining Wang), the National Key Research and Development Program of Ministry of Science and Technology of China in the 13th Five-Year (2016YFC1300402, for Yining Wang), the Non-profit Central Research Institute Fund of Chinese Academy of Medical Sciences (Gran No. 2018RC320004, for Yining Wang), and the National Public Welfare Basic Scientific Research Project of Chinese Academy of Medical Sciences (2017PT32004, for Zhengyu Jin).

Footnote

Conflicts of Interest: All authors have completed the ICMJE uniform disclosure form (available at http://dx.doi.org/10.21037/cdt-20-181). JBS serves as an unpaid editorial board member of *Cardiovascular Diagnosis and Therapy* from Jul 2019 to Jun 2021. The authors have no other conflicts of interest to declare.

Ethical Statement: The authors are accountable for all aspects of the work in ensuring that questions related to the accuracy or integrity of any part of the work are appropriately investigated and resolved. This research was approved by the Institutional Ethnics Committee for Human Research at Peking Union Medical College Hospital (Beijing, China) (No. JS-1470). All subjects have consented to participate in this study.

References

1. Merlini G, Bellotti V. Molecular mechanisms of amyloidosis. New Engl J Med 2003;349:583-96.
2. Maurer MS, Elliott P, Comenzo R, et al. Addressing Common Questions Encountered in the Diagnosis and Management of Cardiac Amyloidosis. Circulation 2017;135:1357-77.
3. Lousada I, Comenzo RL, Landau H, et al. Light Chain Amyloidosis: Patient Experience Survey from the Amyloidosis Research Consortium. Adv Ther 2015;32:920-8.
4. Pereira NL, Grogan M, Dec GW. Spectrum of Restrictive and Infiltrative Cardiomyopathies: Part 1 of a 2-Part Series. J Am Coll Cardiol 2018;71:1130-48.
5. Di Bella G, Pizzino F, Minutoli F, et al. The mosaic of the cardiac amyloidosis diagnosis: role of imaging in subtypes and stages of the disease. Eur Heart J Cardiovasc Imaging 2014;15:1307-15.
6. Knight DS, Zumbo G, Barcella W, et al. Cardiac Structural and Functional Consequences of Amyloid Deposition by Cardiac Magnetic Resonance and Echocardiography and Their Prognostic Roles. JACC Cardiovasc Imaging 2019;12:823-33.
7. Raina S, Lensing SY, Nairooz RS, et al. Prognostic Value of Late Gadolinium Enhancement CMR in Systemic Amyloidosis. JACC Cardiovasc Imaging 2016;9:1267-77.
8. Boynton SJ, Geske JB, Dispenzieri A, et al. LGE Provides Incremental Prognostic Information Over Serum Biomarkers in AL Cardiac Amyloidosis. JACC Cardiovasc Imaging 2016;9:680-6.
9. Fontana M, Pica S, Reant P, et al. Prognostic Value of Late Gadolinium Enhancement Cardiovascular Magnetic Resonance in Cardiac Amyloidosis. Circulation 2015;132:1570-9.
10. Bodez D, Ternacle J, Guellich A, et al. Prognostic value of right ventricular systolic function in cardiac amyloidosis. Amyloid 2016;23:158-67.
11. Wan K, Sun J, Han Y, et al. Right ventricular involvement evaluated by cardiac magnetic resonance imaging predicts mortality in patients with light chain amyloidosis. Heart Vessels 2018;33:170-9.
12. Claus P, Omar AMS, Pedrizzetti G, et al. Tissue Tracking Technology for Assessing Cardiac Mechanics: Principles, Normal Values, and Clinical Applications. JACC

Cardiovasc Imaging 2015;8:1444-60.
13. Illman JE, Arunachalam SP, Arani A, et al. MRI feature tracking strain is prognostic for all-cause mortality in AL amyloidosis. Amyloid 2018;25:101-8.
14. Wan K, Sun J, Yang D, et al. Left Ventricular Myocardial Deformation on Cine MR Images: Relationship to Severity of Disease and Prognosis in Light-Chain Amyloidosis. Radiology 2018;288:73-80.
15. Uzan C, Lairez O, Raud-Raynier P, et al. Right ventricular longitudinal strain: a tool for diagnosis and prognosis in light-chain amyloidosis. Amyloid 2018;25:18-25.
16. Kramer CM, Barkhausen J, Flamm SD, et al. Society for Cardiovascular Magnetic Resonance Board of Trustees Task Force on Standardized Protocols. Standardized cardiovascular magnetic resonance (CMR) protocols 2013 update. J Cardiovasc Magn Reson 2013;15:91.
17. Kumar S, Dispenzieri A, Lacy MQ, et al. Revised prognostic staging system for light chain amyloidosis incorporating cardiac biomarkers and serum free light chain measurements. J Clin Oncol 2012;30:989-95.
18. Schulz-Menger J, Bluemke DA, Bremerich J, et al. Standardized image interpretation and post processing in cardiovascular magnetic resonance: Society for Cardiovascular Magnetic Resonance (SCMR) board of trustees task force on standardized post processing. J Cardiovasc Magn Reson 2013;15:35.
19. Falk RH, Comenzo RL, Skinner M. The systemic amyloidoses. New Engl J Med 1997;337:898-909.
20. Banypersad SM, Moon JC, Whelan C, et al. Updates in cardiac amyloidosis: a review. J Am Heart Assoc 2012;1:e000364.
21. Augustine D, Lewandowski AJ, Lazdam M, et al. Global and regional left ventricular myocardial deformation measures by magnetic resonance feature tracking in healthy volunteers: comparison with tagging and relevance of gender. J Cardiovasc Magn Reson 2013;15:8.
22. Li R, Yang ZG, Xu HY, et al. Myocardial Deformation in Cardiac Amyloid Light-chain Amyloidosis: Assessed with 3T Cardiovascular Magnetic Resonance Feature Tracking. Sci Rep 2017;7:3794.
23. Williams LK, Forero JF, Popovic ZB, et al. Patterns of CMR measured longitudinal strain and its association with late gadolinium enhancement in patients with cardiac amyloidosis and its mimics. J Cardiovasc Magn Reson 2017;19:61.
24. Dungu JN, Valencia O, Pinney JH, et al. CMR-based differentiation of AL and ATTR cardiac amyloidosis. JACC Cardiovasc Imaging 2014;7:133-42.

Cite this article as: Li X, Li J, Lin L, Shen K, Tian Z, Sun J, Zhang C, An J, Jin Z, Vliegenthart R, Selvanayagam JB, Wang Y. Left and right ventricular myocardial deformation and late gadolinium enhancement: incremental prognostic value in amyloid light-chain amyloidosis. Cardiovasc Diagn Ther 2020;10(3):470-480. doi: 10.21037/cdt-20-181

